



## Synthesis, Spectroscopic and Antimicrobial Studies of Some Simple Thiomorpholide–Schiff's base Congeners

Mona Awwad Jaranabi Al-Malki<sup>1</sup>, Nehad Ahmed Abdel Latif<sup>1,2\*</sup>, Mohamed Ramadan El Sayed Aly<sup>1,3\*\*</sup>

<sup>1</sup>Chemistry Department, Faculty of Science, Taif University, 21974-Hawyah-Taif, Kingdom of Saudi Arabia.

<sup>2</sup>Chemistry of Natural Compounds Department, Pharmaceutical and Drug Industries Research Division, National Research Centre, National Research Centre, Dokki, Giza, 12622-Cairo, Egypt.

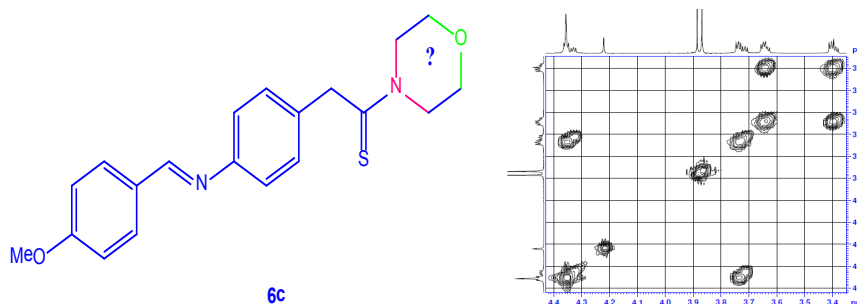
<sup>3</sup>Chemistry Department, Faculty of Science, Port Said University, 42522-Port Said, Egypt.



A SET of eight thiomorpholide-hydrazone conjugates **6a-g** and **7** was prepared in good yield by sequential Willgerodt-Kindler reaction on 4-aminoacetophenone then condensation with the considered aromatic aldehydes. The molecular fragmentation of these conjugates was interpreted by EI-MS. Structure elucidation of these derivatives was further studied using <sup>1</sup>H NMR, COSY, <sup>13</sup>C NMR, Dept-135° and HSQC techniques. The preferred conformation of the morpholine ring was assigned as the <sup>4</sup>C<sub>1</sub> conformation. The COSY spectrum of compound **6c** showed abnormal deshielding of the N(CH<sub>2</sub>)<sub>2</sub> over the O(CH<sub>2</sub>)<sub>2</sub> protons which was explained. *In vitro* antimicrobial screening of these congeners along with standard antibiotics disclosed their moderate activity against *E. coli*, *S. aureus* and *C. albicans*.

**Keywords:** Willgerodt-Kindler, Thiomorpholide, Hydrazone, Spectroscopy, Antimicrobial activity.

### Graphical abstract



### Introduction

Morpholine is a popular fragment in many commercial drugs. The rationale behind that is attributed to the high affinity of the oxygen

atom for hydrogen bonding with many protein receptors *via* donor-acceptor type interactions. Besides, the reduced basicity of the nitrogen atom under the effect of oxygen and the improved

\*Corresponding author e-mail: [nehad\\_km@yahoo.com](mailto:nehad_km@yahoo.com); Tel.: +20 (0)100 74 818 70

\*\*Corresponding author e-mail: [mrea34@hotmail.com](mailto:mrea34@hotmail.com); Tel.: +20 (0) 100 5073049

Received 10/11/2018; Accepted 20/12/2018

DOI: 10.21608/EJCHEM.2018.6165.1517

©2019 National Information and Documentation Center (NIDOC)

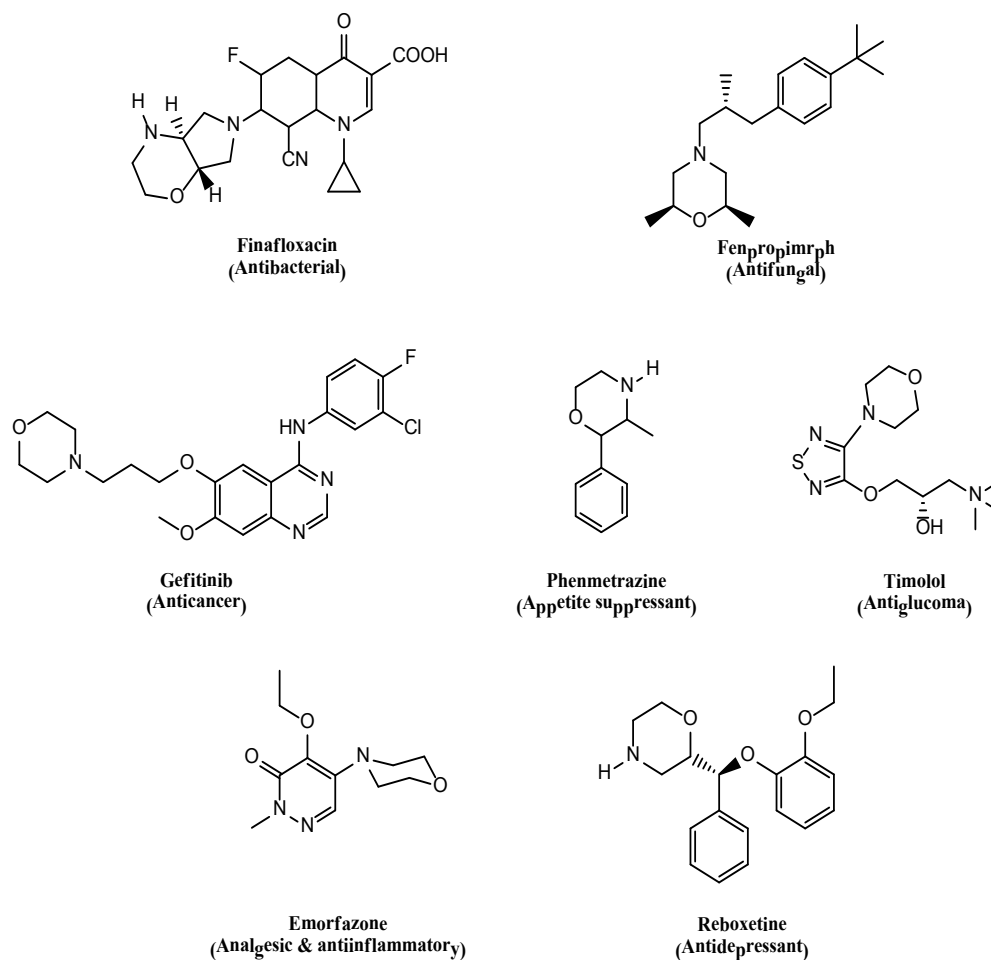


**Fig. 1. Model commercial morpholine based drugs.**

solubility of morpholine containing architectures were important factors in developing their pharmacological potential [1]. Morpholine containing trade mark drugs are used as antibacterial [2], antifungal [2], anticancer [3], appetite suppressant [4], glaucoma relief medications [5], analgesic & antiinflammatories [6], and antidepressants [7] (**Fig. 1**).

Furthermore, morpholine derivatives provided other pharmacologic significances such as antirheumatoid arthritis [8], anti neurodegenerative disorders [9,10], antimalarial [11] and antidiabetic [12,13] activities.

Synthetically, the morpholine nucleus can be tethered *via* direct nucleophilic substitution, Palladium catalyzed *N*-alkylation [14], Copper-Catalyzed C–N Bond formation [15] and from  $\beta$ -amino alcohols [16].

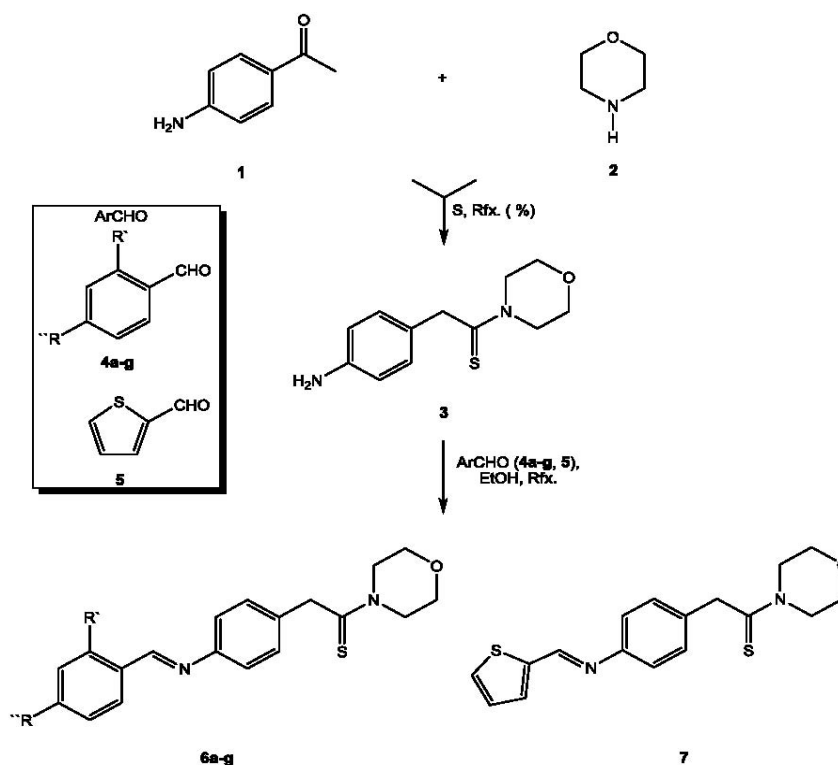
This contribution aimed at attachment of the morpholine ring as thiomorpholide to *Egypt.J.Chem.* **62**, No. 6 (2019)

*p*-aminoacetophenone taking the advantage of Willgerdt-Kindler [17,18] reaction and its modifications [19] then condensation of the amino group with some aldehydes to prepare a set of thiomorpholide-Schiff's base congeners. The cytotoxicity and antimalarial activity of related conjugates were recently disclosed [20]. The antimicrobial activity of the synthesized congeners *in vitro* was evaluated and some stereochemical features of the morpholine moiety were considered by different NMR techniques.

## Results and Discussion

### Chemistry

*p*-Aminoacetophenone was converted into the thiomorpholide substrate **3** (**Scheme 1**) following Willgerdt-Kindler conditions. Thus digestion of *p*-aminoacetophenone with morpholine as reagent and solvent as well in the presence of S under reflux for 6 h afford edintermediate **3** in excellent yield after simple work up. This substrate was pure enough



**Scheme 1.** Synthesis of compounds 6a–g, 7: 6a ( $R'=R''=H$ , 66%); 6b ( $R'=H$ ,  $R''=Me$ , 63%); 6c ( $R'=H$ ,  $R''=OMe$ , 80%); 6d ( $R'=H$ ,  $R''=NMe_2$ , 54%); 6e ( $R'=H$ ,  $R''=Cl$ , 43%); 6f ( $R'=H$ ,  $R''=NO_2$ , 69%); 6g ( $R'=OH$ ,  $R''=H$ , 76%); 7 (60%).

for further use without any requirement for purification. Then, the required Schiff's bases 6a–g and 7 (Scheme 1) were prepared in good yields under ordinary conditions by refluxing with 1.2 equivalents of the appropriate aldehyde in EtOH.

#### Mass spectroscopy

The fragmentation pattern of this series was studied by EI-MS, for instance compounds 6a

(Fig. 2) and 6b (Fig. 3) which showed clearly peaks corresponding to the calculated formula mass of each one.

The mass spectrum of compound 6a (Fig. 2) showed peaks at  $m/z$  values of 238, 194 as base peak, 130, 90 and 86. This peaks, however cannot arise from the same molecular ion, instead three different molecular ions are suggested. If a molecular ion is formed by abstraction of

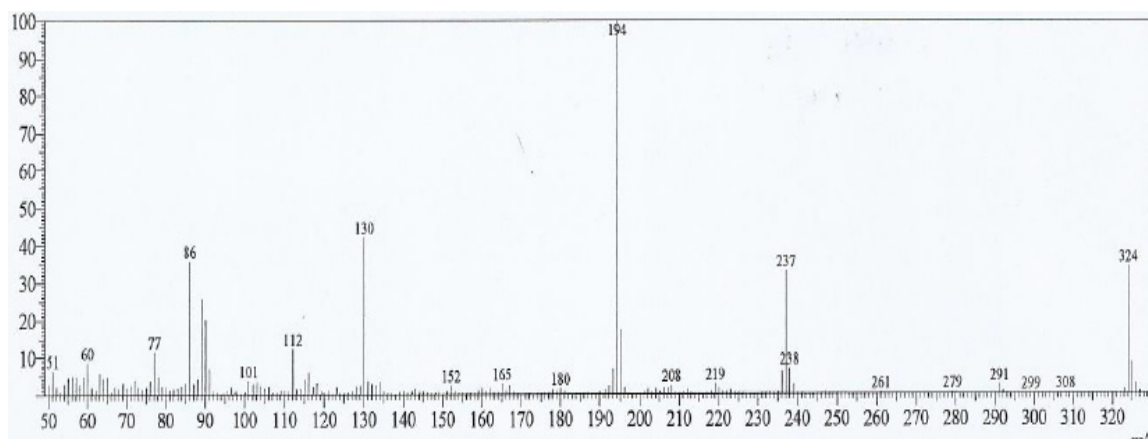
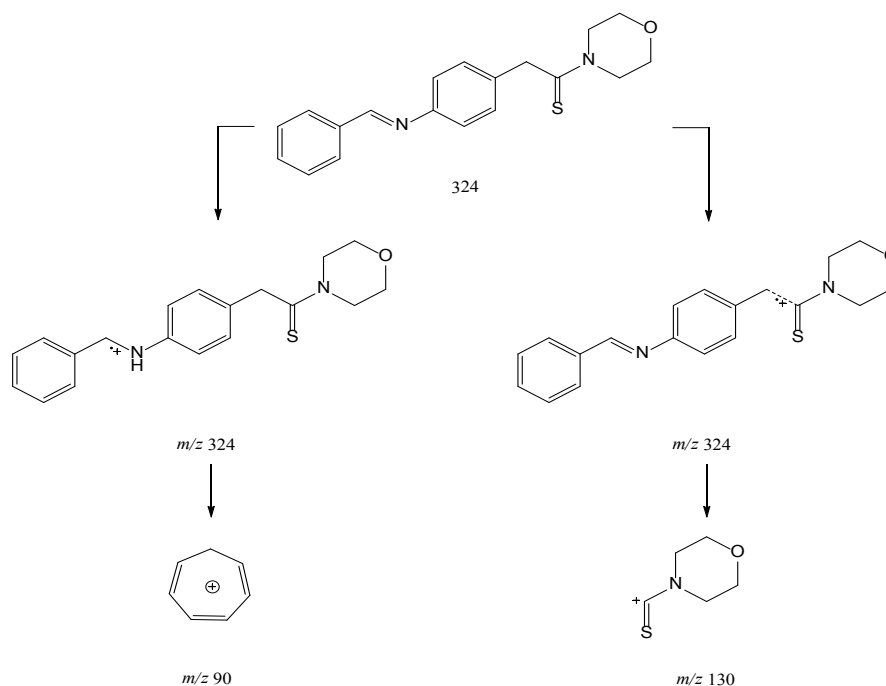


**Fig. 2.** EI-MS spectrum of compound 6a.



**Scheme 2.** Two EI-MS fragmentation patterns of compound **6a**.

an electron at the imine linkage ( $m/z$  324), this might lead to splitting of a tropyllium ion at  $m/z$  90 (**Scheme 2**). Another suggested molecular ion is formed by ionization at the  $\text{CH}_2\text{-C(=S)}$  linkage. Fission of this ionized bond afforded a thiomorpholide fragment at  $m/z$  130.

The third anticipated molecular ion is suggested to be formed by ionization of the morpholinyl  $\text{N-C(=S)}$  linkage. This ion can split in the two possible tracks to afford a morpholinyl cation at  $m/z$  86 or the rest of the molecule as thioketone cation at  $m/z$  238. The later cation loses a CS moiety to afford an ion at  $m/z$  194 as the base peak of the spectrum. Subsequent losing of a methylene group affords a rather molar ion at  $m/z$  180 (**Scheme 3**).

The EI-MS fragmentation pattern of compound **6b** (**Fig. 3**) followed exactly the same mechanism employed in the fragmentation of compound **6a** to afford the  $m/z$  130 ion, a peak at  $m/z$  91 due to the tolyl group as a tropyllium ion and finally, the ions that follows the cleavage morpholine at the  $\text{N-C(=S)}$  bonds (**Scheme 4**).

#### NMR-Characterization

The NMR features of this thiomorpholide-hydrazone series was studied in some detail using  $^1\text{H}$  NMR,  $^{13}\text{C}$  NMR, COSY, HSQC and DEPT-135° techniques.

*Egypt.J.Chem.* **62**, No. 6 (2019)

The confluence of spectral data from these spectra gives deep features about the structure of organic compounds. Thus, in all  $^1\text{H}$  NMR spectra of these Schiff's bases, the imine proton of the Schiff's base moiety was the most deshielded proton due to the anisotropic and inductive effects of the  $\text{C=N}$  linkage. It appeared as singlet at  $\delta \sim 8.5$  ppm in all spectra. An exception is the offset signal of the OH group of the salicylhydrazone **6g** at  $\delta$  13.17 ppm due to intramolecular H-bonding with the imine nitrogen atom.

In the  $^{13}\text{C}$  NMR spectra, the imine carbon was observed at  $\delta \sim 160.31$  ppm. The HSQC gave another evidence for this proton as observed in case of hydrazone **6c** (**Fig. 6**), where a cross-signal arose between the  $^1\text{H}$  signal at 8.5 ppm with the  $^{13}\text{C}$  signal at  $\delta$  160.31 ppm. Meanwhile, this proton did not display any cross signal in the COSY spectrum (**Fig. 5**), and finally its  $^{13}\text{C}$  signal appeared upward polarized in the DEPT-135° spectrum (**Fig. 4**).

The  $^{13}\text{C}$  NMR signal of the thio-group was observed downfield as the most deshielded carbon at  $\delta \sim 200.00$  ppm. Other evidences for this ordinary value of chemical shift for the thio-group included the absence of cross-signals in the HSQC spectrum of **6c** and the DEPT-135° spectrum of the same compound.

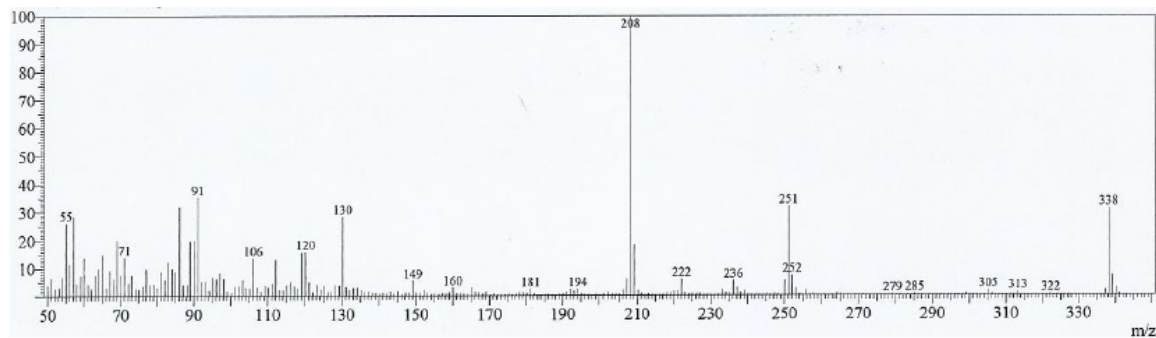
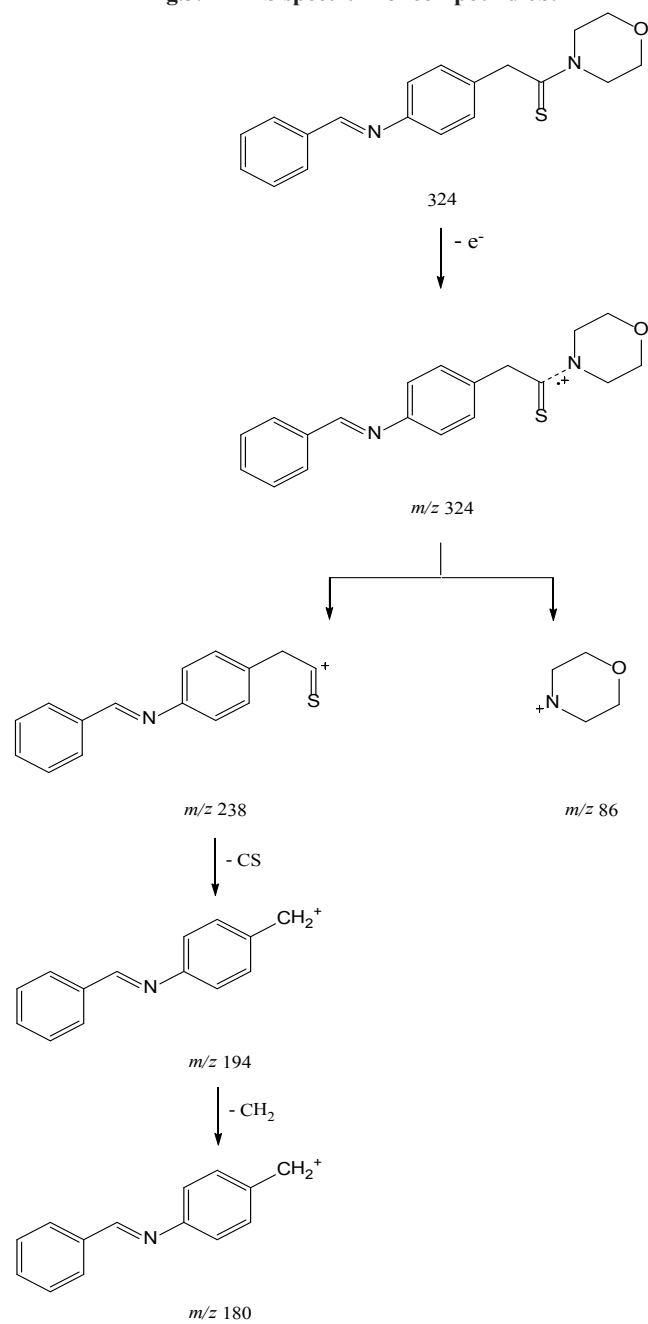
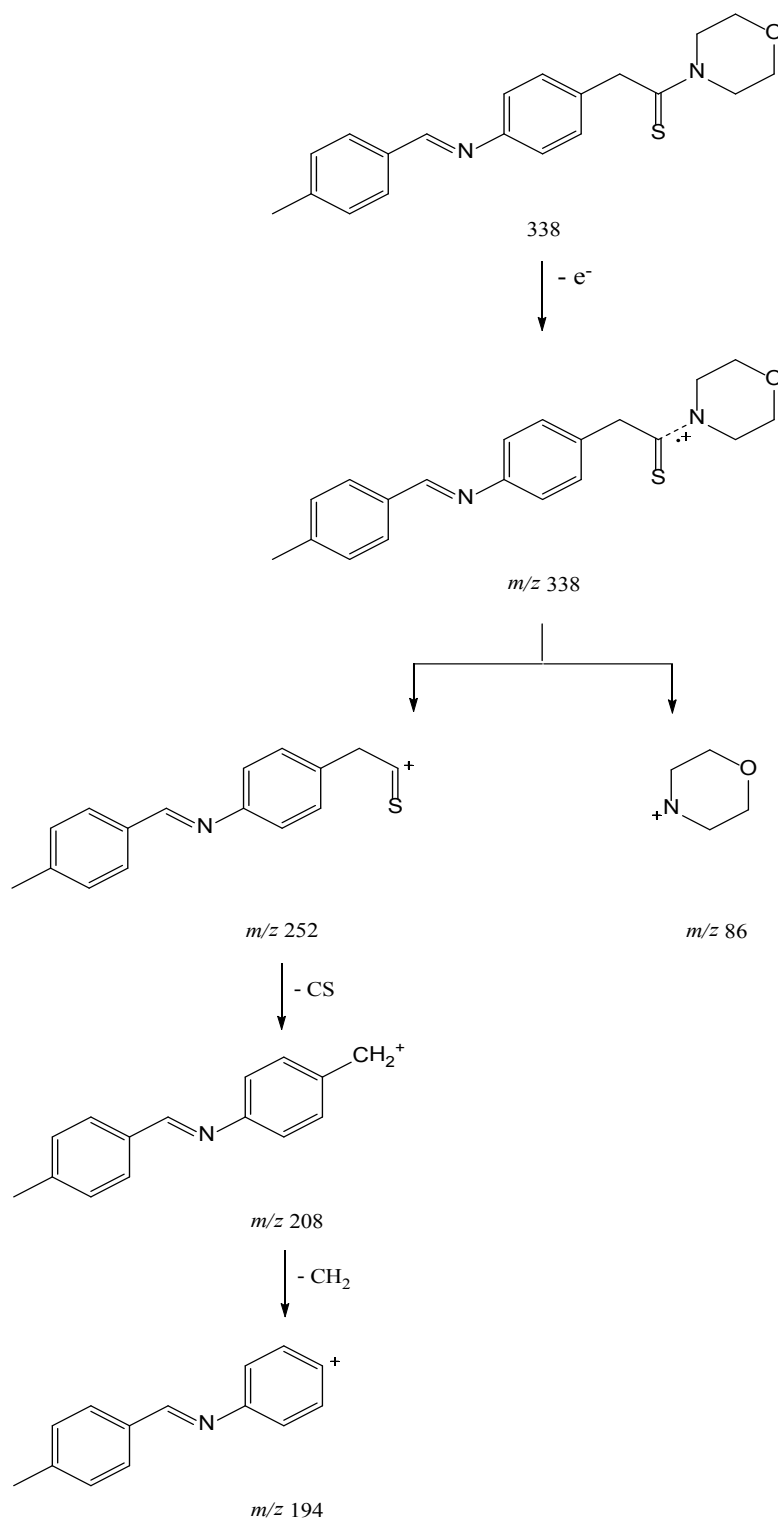


Fig.3. EI-MS spectrum of compound 6b.



Scheme 3. The third route for the MS fragmentation of compound 6a.



Scheme 4. EI-MS fragmentation pattern of compound 6b.

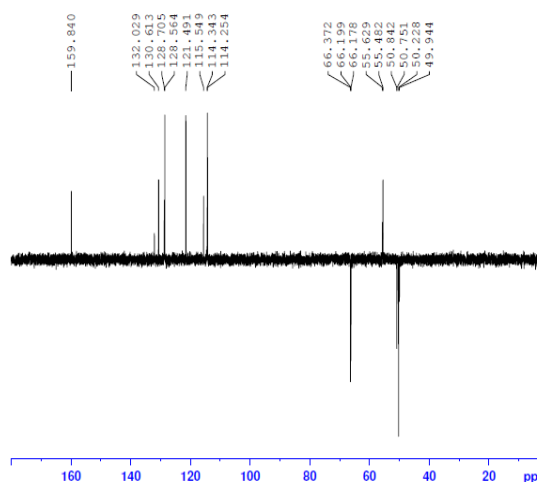


Fig. 4. DEPT-135° spectrum of compound 6c.

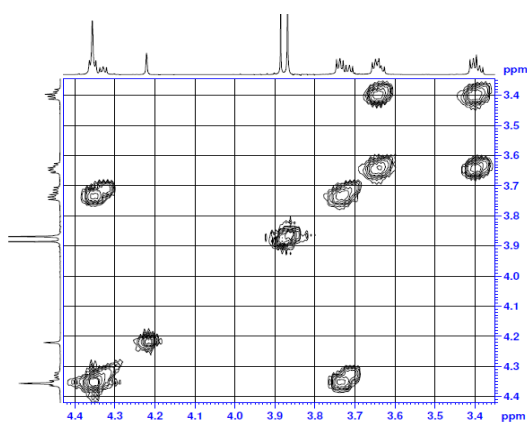


Fig. 5. COSY spectrum of compound 6c.

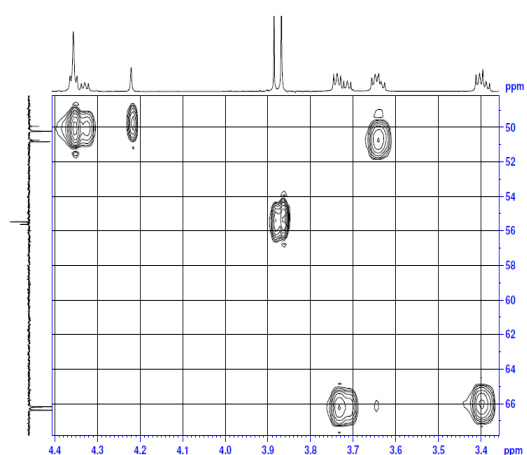


Fig. 6. HSQC spectrum of compound 6c.

On moving from the down-field to the up-field region of the  $^1\text{H}$  NMR spectra of all thiomorpholide Schiff's bases, we denote first that to the best of our knowledge only few spectral analyses were given for the chemical shift of the morpholine ring.

In a report given by Katritzky et al.[21] on some morpholines including even quaternized morpholinyl nitrogen, they demonstrated that the four morpholinyl methylenes are magnetically non-equivalent and appeared at chemical shift values of  $\delta \sim 4.69$  and  $3.82$  ppm for the *O*-linked methylenes, while the values were  $3.39$  and  $2.67$  ppm for the *N*-linked methylenes. Interestingly, they declared from the coupling constant values that the morpholine ring adapts a chair-conformation as deduced from the observed large and small coupling constant values.

Congeners **6a-g** and **7** showed in the downfield region of their  $^1\text{H}$  NMR spectra four triplets at  $\delta \sim 4.36$ ,  $3.72$ ,  $3.65$  and  $3.40$  ppm, respectively. These triplets are related to the four ( $-\text{CH}_2-$ ) groups of the morpholine ring, which are quite obviously magnetically non-equivalent.

The integration of the most deshielded signal at  $\delta 4.36$  ppm was two-fold that of the remaining three triplets, thus denoting that it embodies the singlet of the  $-\text{CH}_2-\text{C}(=\text{S})-$  protons.

At first glance, we thought that the two downfield triplets at  $\delta \sim 4.36$  and  $3.72$  ppm are related to the two *O*-linked methylenes, but the COSY spectrum of **6c** declared another story. As shown in this spectrum, there was a cross-coupling signal between the two down field signals at  $\delta \sim 4.36$  and  $3.72$  ppm which necessitates that they initiate from coupling of one *O*-linked methylene with another *N*-linked congener. Consequently, the remaining two triplets at  $\delta \sim 3.65$  and  $3.40$  ppm are those of the remaining second  $-\text{OCH}_2-$  and  $-\text{NCH}_2-$  of the morpholine ring. Their cross-coupling signals are clear in the COSY spectrum.

A plausible explanation for this deviation in chemical shift of an  $-\text{NCH}_2-$  group and crossing an  $-\text{OCH}_2-$  group may refer to interaction of the nitrogen's lone-pair of electrons with the  $\pi$ -bond electrons of the  $\text{C}=\text{S}$  group which becomes positively polarized. In this way, at least one  $-\text{NCH}_2-$  group become extraordinary deshielded by the magnetic anisotropic effect of the resonance stabilized temporary imine and the inductive effect of its positively polarized nitrogen (Fig. 7).

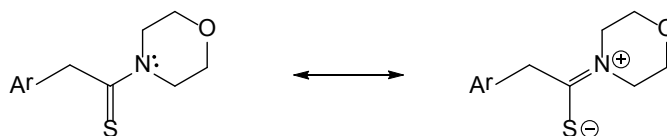


Fig. 7. Tautomerism in the thiomorpholide linkage.

This resonance might be responsible for the extra down-field shift of the singlet arising from the  $-\text{CH}_2-\text{C}(=\text{S})-$  methylene group which become equally affected by this resonance.

Calculation of the coupling constants of lines in each triplet revealed two common values of 4.2, 4.8 and 9.60 Hz. These values suggest a chair conformation of the morpholine ring, where the large coupling value is related to the diaxial-coupling or the coupling between axially oriented hydrogens on vicinal carbons ( $J_{\text{a,a}}$  9.0 Hz), where the dihedral angle is ( $\phi = 180^\circ$ ). Consequently, the small coupling constant values are related to the diequatorial coupling between equatorially oriented vicinal hydrogens which coincidentally equal or of nearby value from the axial-equatorial coupling which gives rise to small coupling constant values ( $J_{\text{e,e}} \sim J_{\text{a,e}} = 4.2$  and 4.8 Hz). This conformation of the morpholine ring is represented in Fig. 8.

As shown in Fig. 8, the  ${}^4\text{C}_1$  conformation is a compatible stereostructure of the morpholine ring as it permits minimum repulsion among the hydrogen atoms and keeps the remainder of the molecule equatorially headed at the morpholine nitrogen atom with the least repulsion with it.

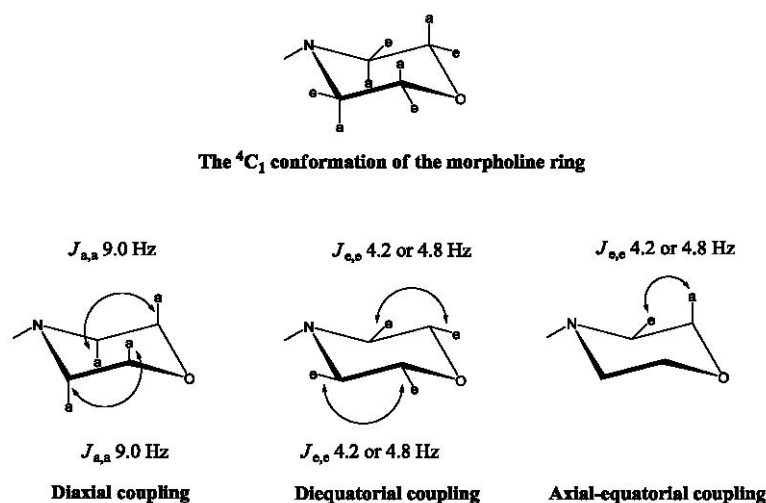
Also, the COSY spectrum declared that the

assigned signal at  $\delta$  3.87 ppm is related to the  $\text{OCH}_3$  group as it is free of cross-coupling signals.

In the aromatic region of compound **6c**, a cross-signal was observed between the two doublets at  $\delta$  7.84 and 6.98 ppm with a common coupling constant value of an AB system  $J_{\text{A,B}}$  8.4 Hz, thus within the characteristic limit of 7–10 Hz. These doublets are related to the anisyl H-2,6 and H-3,5 pairs, respectively. The H-3 and H-5 are more shielded by the mesomeric effect (+*M-effect*) of the methoxy group.

The other two doublets, at  $\delta$  7.33 and 7.17 ppm with a common coupling constant value of  $J_{\text{A,B}}$  7.8 Hz, are related to parent *p*-aminoacetophenone's aryl group. Similarly as in the anisyl ring, the H-3 and H-5 pair are more shielded by some nitrogen's lone-pair interaction with the benzene ring, which shields the *ortho*-protons more than the *meta*-protons.

Comparing the HSQC spectrum of **6c** and the  ${}^{13}\text{C}$  NMR spectrum reveals that the chemical shift of the aromatic C-H carbons at  $\delta$  130.61 and 114.34 ppm belongs to the anisyl AB System carbons, while the signals at  $\delta$  128.56 and 121.49 ppm are attributed to the other carbons of the other aryl AB System.



The  ${}^4\text{C}_1$  conformation of the morpholine ring

Fig. 8. The stereochemistry of the morpholine ring in the morpholine-hydrazone series **6a-g** and **7**.

To deduce the chemical shift of the four *ipso*-carbons, it was necessary to compare the  $^{13}\text{C}$  NMR with the DEPT-135° spectra. The disappearance of the signals at  $\delta$  164.63 and 151.22 ppm in the the DEPT-135° spectrum relates them into the C-4 of the anisyl and that of the other aryl ring, respectively. Similarly, the signal at 133.01 is strongly attributed to the *ipso*-carbon C-1 in both aromatic rings. Interestingly, the still appearing signals can be related easily to impurities that were still in the sample.

Finally, comparison of the HSQC,  $^{13}\text{C}$  NMR and DEPT-135° spectra in the up-field region reveals that the carbon of the  $\text{OCH}_3$  was quite obvious at  $\delta$  55.48 ppm from its up-ward polarization in the DEPT-135° spectrum. All methylene protons including the  $-\text{CH}_2\text{C}(=\text{S})-$  and morpholine's four ( $-\text{CH}_2-$ ) groups were downward polarized in the same spectrum. The carbons of the methylene group in  $\text{CH}_2\text{C}(=\text{S})-$  and two morpholinyl methylenes, originally appeared at  $\delta$  4.35 and 3.63 ppm in the  $^1\text{H}$  NMR spectrum, coincided in the  $^{13}\text{C}$  NMR spectrum on the Y-axis in the HSQC spectrum and appeared at  $\delta$  55.84 and 50.24 ppm.

Another interesting conclusion from the HSQC spectrum is that: the chemical shift of the carbon atoms of the methylene groups of  $^1\text{H}$  chemical shift values of  $\delta$  3.72 and 3.40 ppm were nearly coincide on the Y-axis of  $^{13}\text{C}$  values at  $\delta$  66.37 and 66.20 ppm, respectively.

#### Antimicrobial screening

The antibacterial activity of thiomorpholide-Schiff's bases **6a–g** and **7** was evaluated *in vitro* against *E.coli* (ATCC 11775) (**Fig. 9**) and *S. aureus* (ATTC 12600) (**Fig. 10**) according to the Kirby–Bauer disc diffusion method [22]. As shown in **Fig. 9**, only three derivatives **6d**, **6f**, and

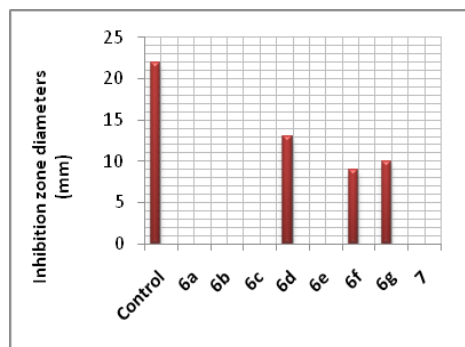


Fig. 9. Inhibition zone diametes against *E. coli*.

**6g** displayed growth inhibitory activity against *E. coli*. Their activities were moderate compared with the positive control (Ampicillin). Normally, Schiff's bases and ligands in general are able to deplete metallo-enzymes from their metal ions that are necessary for their tertiary structures and activities, particularly when the structure and dimensions of the ligand are relevant to penetrate to the enzyme's active site. In case of *E. coli*, the *p*- $\text{NMe}_2$  as in **6d**, the *p*- $\text{NO}_2$  as in **6f**, and the *o*-OH in **6g** were advantageous in imparting the growth inhibitory activity among the considered series. They showed activities of 53%, 40% and 45% of the positive control, respectively.

On moving to *S. aureus* (**Fig. 10**), only two congeners, **6b** and **6d** showed growth inhibitory activity against this bacterial species. Thus, only derivative **6d** of the previous three derivatives retained its activity against *S. aureus* with activity of 61% of the positive control. The *p*-tolyl Schiff's base **6b** showed a growth inhibitory activity of 55% of the positive control.

The antifungal activity of all congeners *in vitro* was evaluated against *A. flavus* (Link) and *Candida albicans* (ATCC 7102) according to the Kirby–Bauer disc diffusion method too. While, *A. flavus* was completely resistant to our series, *C. albicans* was quite sensitive (**Fig. 11**) and it was even more sensitive than the considered bacterial species. The graph clearly displays the activity of all derivatives and fall within the range 41–59% of the positive control (Amphotericin B).

#### Conclusions

In summary, a set of simple thiomorpholide Schiff's base congeners was prepared taking the advantage of Willgerodt-Kindler's reaction. The stereochemistry of the thiomorpholide ring could be declared by NMR spectroscopy with abnormal shift in the COSY spectrum of compound **6c**, that

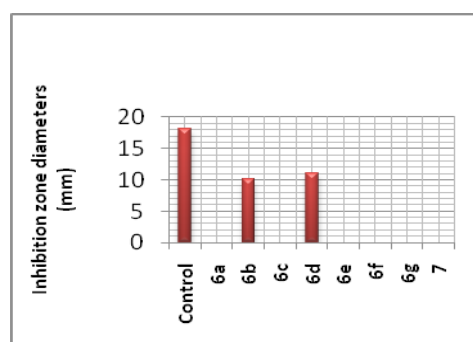


Fig. 10. Inhibition zone diametes against *S. aureus*.

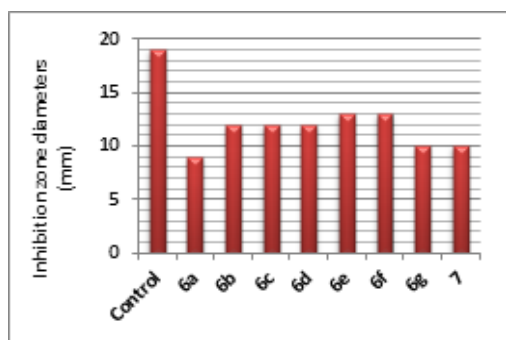


Fig. 11. Inhibition zone diametes against *C. albicans*.

was explained. *C. albicans* was sensitive to the synthesized series compared with *E. coli* and *S. aureus*, while *A. flavus* was resistant. Preparation of more thiomorpholide surrogates and their metal complexes, particularly of the chelating base **6g** might lead to more promising antimicrobial results.

## General Methods

### Chemistry

Melting points were determined on Electrothermal apparatus and are uncorrected. Flash chromatography was carried out on silica gel (Baker, 30–60  $\mu\text{m}$ ). TLC Monitoring tests were carried out using plastic sheets precoated with silica gel 60 F<sub>245</sub> (layer thickness 0.2 mm) purchased from Merck. Spots were visualized by their fluorescence under UV-lamp ( $\lambda$  245 and 366 nm) or staining with iodine vapor, 15 % H<sub>2</sub>SO<sub>4</sub>, KMnO<sub>4</sub>, or Ce(IV)SO<sub>4</sub> in H<sub>2</sub>SO<sub>4</sub>. NMR spectra were recorded on Bruker 600 MHz spectrometer, Central Laboratory, King Abd El Aziz University, Jeddah, Saudi Arabia. IR-spectra were recorded on ATR-Alpha FT-IR Spectrophotometer 400–4000  $\text{cm}^{-1}$ , Chemistry Department, Faculty of Science, Taif University. Mass spectra were recorded on GCMS-QP 1000Ex Shimadzu spectrometers in the Microanalysis unit at Cairo University.

### 2-(4-Amino-phenyl)-1-morpholin-4-yl-ethanethione (3).

A mixture of **1** (3.0 g, 22.2 mmol) and **S** (1.5 g, 47.0 mmol) in **2** (5.0 ml, 49.0 mmol) was heated under gentle reflux for 6h then cooled to ambient temperature. The reaction mixture was coevaporated with toluene in vacuo then purified by flash chromatography from toluene to afford **3** (4.6 g, 87 %) as yellow crystals.  $R_f$  0.28 (toluene), other physical and spectral data were in accordance with the reported one.

*Egypt.J.Chem.* **62**, No. 6 (2019)

### General procedure for the synthesis of (6a-g,7).

A mixture of **3** (1.1g, 4.6 mmol) and the relevant aldehyde **4a–g** or **5** (4.6 mmol) in EtOH (6.0 ml) was stirred under reflux for 3h then cooled spontaneously to ambient temperature. The crystals were filtered, washed with little EtOH and recrystallized from EtOH.

### (E)-2-(4-(Benzylideneamino)phenyl)-1-morpholinoethanethione (6a)

Yield (66%) as yellow crystals; Mp. 126–128 °C;  $R_f$  0.5 (toluene/ethyl acetate, 3:2); <sup>1</sup>H NMR (600 MHz, CDCl<sub>3</sub>):  $\delta$  8.46 (s, 1H, N=CH), 7.91, 7.90 (dd, 2H,  $J$  1.2, 7.2 Hz, H<sub>2</sub>-Ph, H<sub>6</sub>-Ph), 7.49–7.48 (m, 3H, H<sub>3</sub>-Ph, H<sub>4</sub>-Ph, H<sub>5</sub>-Ph), 7.35 (d, 2H,  $J$  9.0 Hz, H<sub>3</sub>-Ar, H<sub>5</sub>-Ar), 7.19 (d, 2H,  $J$  9.0 Hz, H<sub>2</sub>-Ar, H<sub>6</sub>-Ar), 4.37 (m, 4H, OCH<sub>2</sub>, CH<sub>2</sub>C=S), 3.76 (dd, 2H,  $J$  4.8, 5.4 Hz, OCH<sub>2</sub>), 3.66 (dd, 2H,  $J$  4.8, 5.4 Hz, NCH<sub>2</sub>), 3.42 (2d, 2H,  $J$  4.8 Hz, NCH<sub>2</sub>); <sup>13</sup>C NMR (150 MHz, CDCl<sub>3</sub>):  $\delta$  200.03 (C=S), 160.54 (C=N), 150.96 (C<sub>4</sub>-Ar), 136.07 (C<sub>1</sub>-Ph), 133.44, 131.56, 128.86, 128.84, 128.61, 121.50 (10 C<sub>Ar</sub>), 66.38, 66.18 [O(CH<sub>2</sub>)<sub>2</sub>], 50.81 (NCH<sub>2</sub>), 50.22 (NCH<sub>2</sub>, CH<sub>2</sub>CS); EI-MS ( $m/z$ , %) for C<sub>19</sub>H<sub>20</sub>N<sub>2</sub>OS (324.13): 326.10 (M+2, 2.6), 325.10 (M+1, 8.3), 324.15 (M, 34.0), 323.15 (M-H, 1.0), 237.05 (32.8), 236.10 (6.1), 194.10 (100), 130.10 (41.91), 112.10 (12.2), 90.05 (20.0), 86.05 (35.63).

### (E)-2-(4-(4-Methylbenzylideneamino)phenyl)-1-morpholinoethanethione (6b)

Yield (63 %) as yellow crystals; Mp. 136–138 °C;  $R_f$  0.56 (toluene/ethyl acetate, 3:2); <sup>1</sup>H NMR (600 MHz, CDCl<sub>3</sub>):  $\delta$  8.41 (s, 1H, N=CH), 7.78 (d, 2H,  $J$  7.8 Hz, H<sub>2</sub>-Tol, H<sub>6</sub>-Tol), 7.33 (d, 2H,  $J$  8.4 Hz, H<sub>2</sub>-Ar, H<sub>6</sub>-Ar), 7.27 (d, 2H,  $J$  8.4 Hz, H<sub>3</sub>-Tol, H<sub>6</sub>-Tol), 7.17 (d, 2H,  $J$  8.4 Hz, H<sub>3</sub>-Ar, H<sub>5</sub>-Ar), 4.364.34 (m, 4H, OCH<sub>2</sub>, CH<sub>2</sub>CS), 3.73 (dd, 2H,  $J$  4.8, 5.4 Hz, OCH<sub>2</sub>), 3.64 (dd, 2H,  $J$  4.8, 5.4 Hz, NCH<sub>2</sub>), 3.40 (2d, 2H,  $J$  4.8 Hz, NCH<sub>2</sub>), 2.41 (s, 3H, CH<sub>3</sub>); <sup>13</sup>C NMR (150 MHz, CDCl<sub>3</sub>):  $\delta$  199.94 (C=S), 160.37 (C=N), 151.04 (C<sub>4</sub>-Ar), 141.97, 133.44, 133.11, 129.48, 128.76, 128.48, 121.40 (11 C-Ar), 66.27, 66.08 [O(CH<sub>2</sub>)<sub>2</sub>], 50.74 (NCH<sub>2</sub>), 50.12 (NCH<sub>2</sub>, CH<sub>2</sub>CS), 21.58 (CH<sub>3</sub>); ESI-MS ( $m/z$ , %) for C<sub>20</sub>H<sub>22</sub>N<sub>2</sub>OS (338.15): 340.10 (M+2, 2.8), 339.10 (M+1, 7.2), 338.15 (M, 31.2), 337.25 (1.8), 251.10 (31.9), 208.10 (100 %), 130.10 (28.32), 91.10 (35.3), 90.10 (19.9), 86.0 (31.8).

### (E)-2-(4-(4-Methoxybenzylideneamino)phenyl)-1-morpholinoethanethione (6c)

Yield (80%) as yellow crystals; Mp. 130–132 °C;  $R_f$  0.6 (toluene/ethyl acetate, 3:2); <sup>1</sup>H NMR

(600 MHz, CDCl<sub>3</sub>):  $\delta$  8.38 (s, 1H, N=CH), 7.84 (d, 2H, *J* 8.4 Hz, H-2<sub>Anisyl</sub>, H-6<sub>Anisyl</sub>), 7.33 (d, 2H, *J* 7.8 Hz, H-2<sub>Ar</sub>, H-6<sub>Ar</sub>), 7.17 (d, 2H, *J* 7.8 Hz, H-3<sub>Ar</sub>, H-5<sub>Ar</sub>), 6.98 (d, 2H, *J* 8.4 Hz, H-3<sub>Anisyl</sub>, H-5<sub>Anisyl</sub>), 4.36 (m, 4H, CH<sub>2</sub>, CH<sub>2</sub>CS), 3.87 (s, 3H, OCH<sub>3</sub>), 3.74 (t, 2H, *J* 4.2, 4.8 Hz, CH<sub>2</sub>), 3.65 (t, 2H, *J* 4.8 Hz, CH<sub>2</sub>), 3.40 (t, 2H, *J* 4.8, 4.2 Hz, CH<sub>2</sub>); <sup>13</sup>C NMR (150 MHz, CDCl<sub>3</sub>):  $\delta$  200.09 (C=S), 162.39 (C-4<sub>Anisyl</sub>), 159.82 (C=N), 151.22 (C-1<sub>Ar</sub>), 133.01 (C-4<sub>Ar</sub>), 130.61 (C-2<sub>Anisyl</sub>, C-6<sub>Anisyl</sub>), 128.56 (C-2<sub>Ar</sub>, C-6<sub>Ar</sub>), 121.49 (C-3<sub>Ar</sub>, C-5<sub>Ar</sub>), 114.34 (C-3<sub>Anisyl</sub>, C-5<sub>Anisyl</sub>), 66.37, 66.20 [CH<sub>2</sub>CS, 2 (-CH<sub>2</sub>-)], 55.48 (OCH<sub>3</sub>), 50.84 (CH<sub>2</sub>), 50.24 (CH<sub>2</sub>); EI-MS (*m/z*, %) for C<sub>20</sub>H<sub>22</sub>N<sub>2</sub>O<sub>2</sub>S (354.14): 354.92 (M, 0.38), 236.01 (19.8), 191.05 (7.0), 150.06 (14.0), 131.04 (12.7), 106.05 (100), 86.06 (38.3).

*(E)*-2-(4-(4-(dimethylamino)benzylideneamino)phenyl)-1-morpholinoethanethione (6d).

Yield (54%) as dark yellow crystals; Mp. 163–164 °C; *R*<sub>f</sub> 0.43 (toluene/ethyl acetate, 3:2); <sup>1</sup>H NMR (600 MHz, CDCl<sub>3</sub>):  $\delta$  8.31 (s, 1H, N=CH), 7.77 (d, 2H, *J* 7.8 Hz, H-2<sub>Benzylid.</sub>, H-6<sub>Benzylid.</sub>), 7.31 (d, 2H, *J* 8.4 Hz, H-2<sub>Ar</sub>, H-6<sub>Ar</sub>), 7.17 (d, 2H, *J* 7.8 Hz, H-3<sub>Benzylid.</sub>, H-5<sub>Benzylid.</sub>), 6.73 (d, 2H, *J* 8.4 Hz, H-3<sub>Ar</sub>, H-5<sub>Ar</sub>), 3.73–3.36 (m, 4H, OCH<sub>2</sub>, CH<sub>2</sub>CS), 3.74 (t, 2H, *J* 4.8, 5.4 Hz, OCH<sub>2</sub>), 3.65 (t, 2H, *J* 4.8 Hz, NCH<sub>2</sub>), 3.40 (t, 2H, *J* 4.8 Hz, NCH<sub>2</sub>), 3.06 (s, 6H, NMe<sub>2</sub>); <sup>13</sup>C NMR (150 MHz, CDCl<sub>3</sub>):  $\delta$  200.24 (C=S), 160.31 (C=N), 130.59, 128.47, 121.53, 111.59 (12 C-Ar), 66.38, 66.19 [O(CH<sub>2</sub>)<sub>2</sub>], 50.85, 50.33, 50.24 [N(CH<sub>2</sub>)<sub>2</sub>, CH<sub>2</sub>CS], 40.21 (NMe<sub>2</sub>); ESI-MS (*m/z*, %) for C<sub>21</sub>H<sub>25</sub>N<sub>3</sub>OS (367.17): 369.00 (M+2), 368.00 (M+1), 367.00 (M, 3), 149.37 (100%).

*(E)*-2-(4-(4-Chlorobenzylideneamino)phenyl)-1-morpholinoethanethione (6e).

Yield (43%) as faint yellow crystals; Mp. 140–141 °C; *R*<sub>f</sub> 0.61 (toluene/ethyl acetate, 3:2); <sup>1</sup>H NMR (600 MHz, CDCl<sub>3</sub>):  $\delta$  8.42 (s, 1H, N=CH), 7.83 (d, 2H, *J* 8.4 Hz, H-2<sub>ClAr</sub>, H-6<sub>ClAr</sub>), 7.45 (d, 2H, *J* 8.4 Hz, H-3<sub>ClAr</sub>, H-5<sub>ClAr</sub>), 7.35 (d, 2H, *J* 8.4 Hz, H-2<sub>Ar</sub>, H-6<sub>Ar</sub>), 7.18 (d, 2H, *J* 8.4 Hz, H-3<sub>Ar</sub>, H-5<sub>Ar</sub>), 4.38 (m, 4H, OCH<sub>2</sub>, CH<sub>2</sub>CS), 3.75 (t, 2H, *J* 4.8 Hz, OCH<sub>2</sub>), 3.66 (t, 2H, *J* 4.8 Hz, NCH<sub>2</sub>), 3.42 (t, 2H, *J* 4.8 Hz, NCH<sub>2</sub>); <sup>13</sup>C NMR (150 MHz, CDCl<sub>3</sub>):  $\delta$  199.96 (C=S), 158.94 (C=N), 150.56 (C-4<sub>Ar</sub>), 137.56, 134.56, 130.00, 129.15, 128.73, 121.67, 121.49 (11 C-Ar), 66.39, 66.18 [(OCH<sub>2</sub>)<sub>2</sub>], 50.83, 50.21, 50.18 [N(CH<sub>2</sub>)<sub>2</sub>, CH<sub>2</sub>CS]; ESI-MS (*m/z*, %) for C<sub>19</sub>H<sub>19</sub>ClN<sub>2</sub>OS (358.09): 359 (M+1), 358.0 (M, 3), 331.21 (100%).

*(E)*-1-Morpholino-2-(4-(4-nitrobenzylideneamino)phenyl)ethanethione (6f).

Yield (69 %) as faint yellow crystals; Mp. 146–148 °C; *R*<sub>f</sub> 0.53 (toluene/ethyl acetate, 3:2); <sup>1</sup>H NMR (600 MHz, CDCl<sub>3</sub>):  $\delta$  8.56 (s, 1H, N=CH), 8.33 (d, 2H, *J* 9.0 Hz, H-3<sub>NitroAr</sub>, H-5<sub>NitroAr</sub>), 8.07 (d, 2H, *J* 9.0 Hz, H-2<sub>NitroAr</sub>, H-6<sub>NitroAr</sub>), 7.40 (d, 2H, *J* 8.4 Hz, H-2<sub>Ar</sub>, H-6<sub>Ar</sub>), 7.25 (d, 2H, *J* 8.4 Hz, H-3<sub>Ar</sub>, H-5<sub>Ar</sub>), 4.38–4.36 (m, 4H, OCH<sub>2</sub>, CH<sub>2</sub>CS), 3.76 (t, 2H, *J* 4.8 Hz, OCH<sub>2</sub>), 3.67 (t, 2H, *J* 4.2, 4.8 Hz, NCH<sub>2</sub>), 3.40 (t, 2H, *J* 4.2, 4.8 Hz, NCH<sub>2</sub>); <sup>13</sup>C NMR (150 MHz, CDCl<sub>3</sub>):  $\delta$  199.75 (C=S), 157.44 (C=N), 149.82 (C-4<sub>NitroAr</sub>), 141.46 (C-4<sub>Ar</sub>), 134.75, 129.45, 128.84, 124.08, 121.63 (10 C<sub>Ar</sub>), 66.40, 66.19 [(O(CH<sub>2</sub>)<sub>2</sub>), 50.84, 50.21, 50.10 [N(CH<sub>2</sub>)<sub>2</sub>, CH<sub>2</sub>CS]; ESI-MS (*m/z*, %) for C<sub>19</sub>H<sub>19</sub>N<sub>3</sub>O<sub>3</sub>S (369.11): 370 (M+1), 369.1 (M), 119.21, 149.34 (100%).

*(E)*-2-(4-(2-Hydroxybenzylideneamino)phenyl)-1-morpholinoethanethione (6g).

Yield (76%) as dark yellow crystals; Mp. 150–152 °C; *R*<sub>f</sub> 0.53 (toluene/ethyl acetate, 3:2); <sup>1</sup>H NMR (600 MHz, CDCl<sub>3</sub>):  $\delta$  13.17 (br.s, 1H, OH), 8.62 (s, 1H, N=CH), 7.40–7.38 (m, 3H), 7.25 (d, 2H, *J* 8.4 Hz), 7.02 (d, 1H, *J* 8.4 Hz), 6.95 (t, 1H, *J* 7.2, 7.8 Hz), 4.37 (t, 2H, *J* 4.8 Hz, OCH<sub>2</sub>), 4.37 (s, 2H, CH<sub>2</sub>CS), 3.76 (t, 2H, *J* 4.2, 5.4 Hz, O(CH<sub>2</sub>)<sub>2</sub>), 3.66 (t, 2H, *J* 4.2, 5.4 Hz, N(CH<sub>2</sub>), 3.46 (t, 2H, *J* 4.8 Hz, NCH<sub>2</sub>); <sup>13</sup>C NMR (150 MHz, CDCl<sub>3</sub>):  $\delta$  199.76 (C=S), 162.73 (C-OH), 161.14 (C=N), 147.47 (C-4<sub>Ar</sub>), 134.52, 133.31, 132.36, 128.91, 121.75, 119.17, 117.30 (10 C-Ar), 66.40, 66.19 [(O(CH<sub>2</sub>)<sub>2</sub>), 50.82, 50.19, 50.03 [N(CH<sub>2</sub>)<sub>2</sub>, CH<sub>2</sub>CS]; ESI-MS (*m/z*, %) for C<sub>19</sub>H<sub>20</sub>N<sub>2</sub>O<sub>2</sub>S (340.12): 342 (M+2), 341 (M+1), 340 (M), 325.51, 341.36, 64.30 (100%).

*(E)*-1-Morpholino-2-(4-(thiophen-2-ylmethyleneamino)phenyl)ethanethione (7)

Yield (60 %) as yellowish brown crystals; Mp. 118–120 °C; *R*<sub>f</sub> 0. (toluene/ethyl acetate, 3:2); <sup>1</sup>H NMR (600 MHz, CDCl<sub>3</sub>):  $\delta$  8.56 (s, 1H, N=CH), 7.51 (d, 1H, *J* 4.8 Hz, H-5<sub>Thioph.</sub>), 7.48 (d, 1H, *J* 3.6 Hz, H-3<sub>Thioph.</sub>), 7.32 (d, 2H, *J* 8.4 Hz, H-2<sub>Ar</sub>, H-6<sub>Ar</sub>), 7.18 (d, 2H, *J* 8.4 Hz, H-3<sub>Ar</sub>, H-5<sub>Ar</sub>), 7.13 (dd, 1H, *J* 3.6, 4.8 Hz, H-4<sub>Thioph.</sub>), 3.35 (2d, 2H, *J* 4.8 Hz, OCH<sub>2</sub>), 3.35 (s, 2H, CH<sub>2</sub>CS), 3.72 (t, 2H, *J* 4.8, 5.4 Hz, OCH<sub>2</sub>), 3.64 (t, 2H, *J* 4.2, 5.4 Hz, NCH<sub>2</sub>), 3.39 (t, 2H, *J* 4.2, 5.4 Hz, NCH<sub>2</sub>); <sup>13</sup>C NMR (150 MHz, CDCl<sub>3</sub>):  $\delta$  199.97 (C=S), 153.15 (C=N), 150.32 (C-4<sub>Ar</sub>), 142.70 (C-2<sub>Thioph.</sub>), 133.52, 132.46, 128.60, 127.85, 121.62 (8 C<sub>Ar</sub>), 66.37,

66.17 [O(CH<sub>2</sub>)<sub>2</sub>], 50.84, 50.22 [N(CH<sub>2</sub>)<sub>2</sub>, CH<sub>2</sub>CS]; ESI-MS (*m/z*,%) for C<sub>17</sub>H<sub>18</sub>N<sub>2</sub>OS<sub>2</sub> (330.09): 332 (M+2), 331 (M+1), 330 (M).

#### Antimicrobial screening

The antimicrobial activity of was determined using a modified Kirby–Bauer disc diffusion method. Ampicillin and Amphotericin B were used as bacterial and fungal positive controls, respectively, while DMSO was used as solvent and negative control as well. Four microbial species were considered, *E. coli* (G<sup>-</sup> bacteria), *S. aureus* (G<sup>+</sup> bacteria), *A. flavus* (filamentous fungi) and *C. albicans* (yeast).

Briefly, 100 µl of the test organism were grown in 10 ml of fresh media until they reached a count of 10<sup>8</sup> cells/ml for bacteria and 10<sup>5</sup> cells/ml for fungi. 100 µl of the microbial suspension was spread onto MullerHinton agar plates. Paper discs (Sceicher & Schull, Spain) with a diameter of 8.0 mm were impregnated 10 µl of the test compound (4.0 mM) and controls were treated similarly. Plates were incubated for 48 h at 35–37 °C for bacterial strains, 25 °C for *A. flavus* and 30 °C for *C. albicans*. Inhibition zone diameters were measured with slipping calipers.

#### References

- Shcherbatuik, A. V. et al., Synthesis of 2- and 3-trifluoromethylmorpholines: useful building blocks for drug discovery. *Tetrahedron*, **69**, 3796–3804 (2013).
- Pal'Chikov, V. A., Morpholines. Synthesis and Biological Activity. *Russ. J. Org. Chem.* **49**(6), 787–814 (2013).
- Burotto, M.; Manasanch, E. E.; Wilkerson J.; Fojo T., Gefitinib and erlotinib in metastatic non-small cell lung cancer: a meta-analysis of toxicity and efficacy of randomized clinical trials. *Oncologist*. **20**(4), 400–410 (2015).
- Rothman, R. B.; Baumann, M. H., Therapeutic potential of monoamine transporter substrate. *Curr. Top. Med. Chem.* **6**(17), 1845–1859 (2006).
- Sena, D. F.; Ramchand, K.; Lindsley, K., Pharmacological interventions for smoking cessation: an overview and network meta-analysis. *Cochrane Database Syst Rev.* **2013**, CD 006539.
- Asif, M., Biological Potential of Fluoro- Benzene Analogs. *Ann. Med. Chem. Res.* **2**(1), 1015–2017 (2016).
- Ates, M.A., Durmaz, O., Bez, Y, Reboxetine Induced Painful Ejaculation: A Case Report, *Journal of Mood Disorders* **1**(4), 166-8 (2011)
- Lou, Y.; Han, X.; Kuglstatte, A.; Kondru, R. K.; Sweeney, Z. K.; Soth, M.; McIntosh, J.; Litman, R.; Suh, J.; Kocer, B.; Davis, D.; Park, J.; Frauchiger, S.; Dewdney, N.; Zecic, H.; Taygerly, J. P.; Sarma, K.; Hong, J.; Hill, R. J.; Gabriel, T.; Goldstein, D. M.; Owens, T. D., Structure-Based Drug Design of RN486, a Potent and Selective Bruton's Tyrosine Kinase (BTK) Inhibitor, for the Treatment of Rheumatoid Arthritis. *J. Med. Chem.* **58**, 512–516 (2015).
- Henderson J. L. Henderson J. L.; Kormos B. L.; Hayward M. M.; Coffman K. J.; Jasti J.; Kurumbail R. G.; Wager T. T.; Verhoest P. R.; Noell G. S.; Chen Y.; Needle E.; Berger Z.; Steyn S. J.; Houle C.; Hirst W. D.; Galatsis P. Discovery and Preclinical Profiling of 3-[4-(Morpholin-4-yl)-7H-pyrrolo[2,3-d]pyrimidin-5-yl]benzotrile (PF-06447475), a Highly Potent, Selective, Brain Penetrant, and in Vivo Active LRRK2 Kinase Inhibitor. *J., Med. Chem.* **58**, 419–432 (2015).
- Huang, X.; Pissarnitski, D.; Li, H.; Asberom, T.; Josien, H.; Zhu, X.; Vicarel, M.; Zhao, Z.; Rajagopalan, M.; Palani, A.; Aslanian, R.; Zhu, Z.; Greenlee, W., Efficient synthesis and reaction pathway studies of novel fused morpholine oxadiazolines for use as gamma secretase modulators. *Tetrahedron Lett.* **53**, 6451–6455 (2012).
- Figueiras, M.; Coelho, L.; Wicht, K. J.; Santos, S. A.; Lavrado, J.; Gut, J.; Rosenthal, P. J.; Nogueira, F.; Egan, T. J.; Moreira, R.; Paulo, A., N10,N11-di-alkylamine indolo[3,2-b]quinolines as hemozoin inhibitors: Design, synthesis and antiplasmodial activity. *Bioorg. Med. Chem.* **23**, 1530–1539 (2015).
- Kar K.; Kar K.; Krithika U.; Mithuna; Basu P.; Santhosh Kumar S.; Reji A.; Prashantha Kumar B. R., Design, synthesis and glucose uptake activity of some novel glitazones. *Bioorg. Chem.* **56**, 27–33.(2014).
- Burland P.A., Synthesis and glycosidase inhibitory profiles of functionalised morpholines and oxazepanes. *Bioorg. Med. Chem.* **19**, 5679–5692 (2011).
- Nowak M.; Malinowski Z.; Józwiak A.; Fornal E.; Błaszczuk A.; Kontek R., Substituted benzoquinazolinones. Part 1: Synthesis of

- 6-aminobenzo[*h*]quinazolinones via Buchwald–Hartwig amination from 6-bromobenzo[*h*]quinazolinones. *Tetrahedron* **70**, 5153–5160 (2014).
15. Fodor A.; Kiss A.; Debreczeni N.; Hell Z.; Gresits I., A simple method for the preparation of propargylamines using molecular sieve modified with copper(II). *Org. Biomol. Chem.* **8**, 4575–4581.(2010).
16. Testa M. L.; Zaballos E.; Zaragoza R. J., Reactivity of  $\beta$ -amino alcohols against dialkyl oxalate: synthesis and mechanism study in the formation of substituted oxalamide and/or morpholine-2,3-dione derivatives. *Tetrahedron*, **68**, 9583–9591. (2012).
17. Willgerodt, C., verschlechtern sich die Ausbeuten drastisch durch die Zunahme der Kettenlänge der Alkylreste. *Ber. Dtsch. Chem. Ges.* **21**, 534–536. (1888).
18. Kindler, K., Studien über den Mechanismus chemischer Reaktionen. Erste Abhandlung. Reduktion von Amidinen und Oxydation von Aminen. *Liebigs Ann. Chem.* **431**, 187–207. (1923).
19. Priebbenow, D. L.; Bolm, C., Studien über den Mechanismus chemischer Reaktionen. Erste Abhandlung. Reduktion von Amidinen und Oxydation von Aminen. *Chem. Soc. Rev.* **42**, 7870–7880. (2013).
20. Jarrahpour, A.; Shirvani, P.; Sharghi, H.; Aberi, M.; Sinou, V.; Latour, C.; Brunel, J.M., Synthesis of novel mono- and bis-Schiff bases of morpholine derivatives and the investigation of their antimalarial and antiproliferative activities *Med. Chem. Res.*, **24**(12), 4105–4112 (2015).
21. Katritzky, A. R.; Akhmedov, N. G.; Yang, H.; Hall, C. D.,  $^1\text{H}$  and  $^{13}\text{C}$  NMR spectra of *N*-substituted morpholines. *Magn. Reson. Chem.* **43**, 673–675 (2005).
22. Bauer, A. M.; Kirby, W. M.; Sherris, C.; Turck, M. A. J.; Antibiotic susceptibility testing by a standardized single disk method. *Clin. Pathol.* **45**, 493–496. (1966).

### تشبيد ودراسات طيفية ومضاده للميكروبات على بعض مترافقات ثيومورفولاييد مع قواعد شيف

منى عواض جار النبي المالكي<sup>1</sup>، نهاد أحمد عبد اللطيف<sup>2</sup>، محمد رمضان السيد علي<sup>3</sup>  
<sup>1</sup>قسم الكيمياء – كلية العلوم – جامعة الطائف – الطائف – المملكة العربية السعودية.  
<sup>2</sup>قسم كيمياء المركبات الطبيعية – شعبه بحوث الصناعات الصيدليه والدوائيه – المركز القومي للبحوث – الدقي – القاهرة – مصر.  
<sup>3</sup>قسم الكيمياء – كلية العلوم – جامعة بورسعيد – بورسعيد – مصر.

تم في هذا البحث تشبيد المجموعه **6a-g & 7** من مترافقات ثيومورفولاييد قاعده شيف بتسلسل تفاعلات فيلجروديت - كيندلر على مركب -4 أمينو اسيتوفينون ثم التكايف مع مجموعه من الالدهيدات العطريه.

وقد تمت دراسة التفسير الجزيئي لتلك المركبات في مطياف الكتله وتفسيره. كما تمت دراسة تركيبها الدقيق بأستفاضه باستخدام تقنيات الرنين النووي المغناطيسي الهيدروجيني والكربوني المتعدده والتي تم من خلالها تحديد الشكل المفصل لحلقة المورفولين وهو التركيب  $\text{C}_1^4$ . وقد أظهر الطيف الهيدروجيني في اتجاهين سلوكا غير معتاد للمركب **6c** حيث كانت مجموعتي الميثيلين المرتبطتين بذرة نيتروجين حلقة المورفولين ذات ازاحه كيميائيه أعلى من تلك المرتبطه بذره الاكسجين في ذات الحلقه وتم تفسير ذلك.

وبدراسة النشاط المضاد للميكروبات خارج الكائن وبالمقارنه بالمضادات الحيويه القياسيه فقد تبين نشاط تلك المركبات المتوسط تجاه الكائنات الدقيقه موضع الدراسه.